JOURNAL OF AIRCRAFT
Vol. 33, No. 5, September–October 1996

Subsonic Unsteady Aerodynamics Caused by Gusts Using the Indicial Method

J. Gordon Leishman*
University of Maryland, College Park, Maryland 20742

Indicial approximations are derived for the lift on an airfoil penetrating a stationary sharp-edge gust in two-dimensional subsonic flow. Using an assumed exponential form, the approximations have been generalized in terms of Mach number alone by means of an optimization algorithm where certain coefficients of the approximations are free parameters. The optimization is subject to prescribed constraints in terms of the initial and asymptotic behavior of the gust response, and by requiring the response closely match the known exact solutions given by subsonic linear theory at earlier values of time. An alternative approximation is obtained by using results from a direct numerical simulation of the gust problem using computational fluid dynamcs (CFD). For an airfoil–vortex interaction problem, comparisons were made with experimental data and CFD results. Finally, the indicial method was integrated into a three-dimensional rotor simulation, and the near- and far-field acoustics were computed using the Ffowcs Williams–Hawkins equation. Good agreement was found with simultaneously measured airloads and acoustics data.

Nomenclature

a = sonic velocity, ms^{-1}
C_n^g = normal force coefficient caused by gust
c = rotor blade chord, m
E = complete elliptic integral of the second kind
$E'(\Psi)$ = incomplete elliptic integral of the second kind
$F'(\Psi)$ = incomplete elliptic integral of the first kind
G_i = coefficients of sharp-edged gust function
g_i = exponents of sharp-edged gust function
J = cost function
K = complete elliptic integral of the first kind
k = modulus of elliptic integrals
k_g = gust reduced frequency
$l_{\mathcal{R}}$ = force on fluid in direction of $\mathcal{R}$, N
M = local freestream Mach number
$M_{\mathcal{R}}$ = relative Mach number between source and receiving point
p = Laplace variable
p' = fluctuating pressure, Pa
R = rotor radius, m
$\mathcal{R}$ = distance from source to observer, m
r = radial distance from vortex center, m
r_c = vortex core radius, m
S = blade area, m^2
s = nondimensional distance in semichords, $2Vt/c$
t = time, s
V = local (freestream) velocity, ms^{-1}
V_g = gust convection velocity, ms^{-1}
V_θ = tangential velocity, ms^{-1}
v_n = normal perturbation velocity, ms^{-1}
w = weighting term
w_g = gust velocity normal to airfoil, ms^{-1}
x_v, y_v, z_v = position of vortex, m
x, y = airfoil coordinate system, measured from leading edge, m
Z_i = aerodynamic deficiency functions
z_i = aerodynamic states
α = angle of attack, rad
α_e = effective angle of attack, rad
β = Glauert factor, $\sqrt{1 - M^2}$
Γ = vortex strength (circulation), m^2/s
$\hat{\Gamma}$ = nondimensional vortex strength, Γ/Vc
Δ = incremental quantity
ΔC_p = differential pressure coefficient
λ = gust speed ratio, $V/(V + V_g)$
ρ = air density, kg m^{-3}
σ = dummy variable of integration
τ = retarded time, s
ϕ = indicial response function
Ψ = argument of elliptic integrals
ψ_g = sharp-edged gust function
ω_g = gust frequency, rad/s

Introduction

THE accurate prediction of the unsteady forces and moments induced on airfoils encountering gusts and vortices plays a critical role in the aeroelasticity and acoustics of aircraft wings, rotors, and turbomachines. Gust problems are particularly acute for helicopters and tilt-rotors, where it is known that the blades can frequently encounter the intense velocity gradients generated by tip vortices trailed from previous blades. These blade vortex interactions (BVI) have been identified as a significant source of unsteady aerodynamic loading and a major contributor to rotor noise.[1,2]

Extensive research has provided a good amount of fundamental knowledge on the BVI phenomenon, and has led to an increased appreciation of the complex physical nature of the flow and the difficulties in its prediction.[3–6] Accurate predictions of BVI airloadings and the related rotor noise are becoming more critical aspects of the basic rotor design process to meet stringent noise certification requirements. To this end, it must be appreciated that accurate prediction of BVI aeroacoustic phenomena will involve blade structural dynamic and aerodynamic modeling as a fully closed-loop system, including free-wake modeling and perhaps the implementation of active controls. This places serious constraints on the allowable levels of unsteady aerodynamic modeling. Even when the aerodynamics model may include some level of unsteady and/or compressibility modeling, the approach used in modern rotor codes such as CAMRAD[7] or UMARC[8] do not completely distinguish the aerodynamic effects at the blade element level caused by the wake-induced velocity from the aerodynamic effects be-

Received Oct. 1, 1995; revision received May 9, 1996; accepted for publication May 10, 1996.

*Associate Professor, Glenn L. Martin Institute of Technology, Department of Aerospace Engineering. Senior Member AIAA.

cause of changes in angle of attack and pitch rate. The former can be considered as a series of gusts through which the blade section penetrates, whereas the latter will be because of blade motion such as flapping, pitch control inputs for trim, and blade torsional response. Each produces a different source of unsteady aerodynamic loading and time–history. Therefore, not only is the lack of distinction between gust encounters and changes in angle of attack or pitch rate fundamentally incorrect, but it may lead to erroneous predictions of the unsteady airloads and resulting acoustics.

Although the practical difficulties in predicting accurately the unsteady aerodynamics caused by gusts and wake vortices in the rotor environment has been recognized before,[9,10] it has not been fully resolved. The increasing trend toward the development of active rotor control technologies such as blade-mounted trailing-edge flaps for possible BVI noise and vibration reduction[11,12] means that improved and validated unsteady aerodynamic models with a more rigorous physical basis must be developed. Furthermore, if successful active control strategies for vibration and noise reduction are to be developed, then the unsteady aerodynamics and acoustics must be written in an appropriate numerical form that will lend itself to straightforward implementation in a control algorithm.

The basis of the present approach is the indicial response method. This is the response of the aerodynamic flowfield to a step change in a set of defined boundary conditions such as a step change in airfoil angle of attack, a step change in pitch rate about some axis, or a step change in control surface deflection (such as a tab or flap). A good review of the indicial concept is given by Tobak and Schiff.[13] If the indicial response can be computed, then the response to an arbitrary motion of the airfoil or control surface can be found by Duhamel superposition. If the linearity of the physics over the required range of conditions can be justified, then the advantage of the indicial method is a tremendous saving in computational cost over performing separate flowfield calculations.

A particularly useful application of the indicial method is in the calculation of gust-induced airloads. The unsteady effects produced on airfoils arise primarily because of the vertical velocity between the disturbance (the gust field) and the airfoil surface. In linear theory, this component is used to satisfy the boundary conditions of flow tangency on the airfoil surface. Unsteady effects caused by the in-plane component of the gust velocity can usually be ignored since horizontal disturbances produce a quasisteady effect to a first-order.[14,15] However, nonlinear effects may be a more significant factor under transonic conditions, especially if the blade passes close to the core of a vortex. Here, the upstream propagation of unsteady wake effects toward the leading edge of the airfoil will appear as increased phase lags because of the existence of a supersonic pocket.

Using linear theory, classical incompressible solutions for the stationary sharp-edged gust problem were obtained by Küssner,[16] and von Kármán and Sears.[17] For the general gust problem in incompressible flow, Duhamel superposition can be used with the Küssner function $\psi_g(s)$ to find the aerodynamic loads caused by an arbitrary stationary gust field. For the traveling vertical gust case, the problem was solved numerically for incompressible flow by Miles,[18] and for subsonic flows by Drischler and Diedrich[19] in terms of the parameter $\lambda = V/(V + V_g)$. In the incompressible case as the propagation speed of the traveling gust increases from zero to ∞ (λ decreases from one to zero), the solution changes from the Küssner result to the Wagner result,[20] with a variety of intermediate transitional results being obtained.[18] The equivalent sharp-edge gust solutions for the subsonic case can be obtained only approximately, and even then they are not easily represented in a practical computational form. However, in the rotor environment, the convected wake velocities are generally much lower than the local blade element velocity, and so the assumption that $\lambda \approx 1$ is usually valid and the stationary sharp-edged gust result can be assumed. This produces a justifiable level of simplification in the unsteady aerodynamic modeling that retains the efficiency necessary for a comprehensive rotor aeroacoustics simulation.

The approach used in the present article is built partly on the subsonic linear analysis of Lomax,[21,22] and deals with the problem of formulating a practical unsteady aerodynamic model for predicting BVI-type airloads in the rotor environment. A first objective is to construct a set of generalized sharp-edge gust functions that are valid for linearized subsonic flow, and can be applied through indicial principles to the calculation of airloads caused by arbitrary gusts. Clearly, if developed into an appropriate generalized form, numerical analyses that are based on subsonic linearized unsteady aerodynamic models are a valuable first step toward an improved prediction capability. This is justified in the present work using results from BVI experiments as well as direct simulations of the gust and BVI problems using a Navier–Stokes/Euler computational fluid dynamics (CFD) solver. It is also intended to produce an economical numerical method suitable for preliminary parametric studies of the acoustic effects of airfoil–vortex interaction and possible means of alleviation by means of active blade control.[11,23]

Analysis

Two-Dimensional Exact Subsonic Linear Theory

Unlike the classical Küssner sharp-edged gust function, there are no equivalent exact solutions for the gust available in the subsonic case, at least not over the entire time domain of interest. Compared to the indicial angle-of-attack result, which has a finite (noncirculatory) value at $s = 0$ as given by linear piston theory,[20] the gust solution starts at zero lift at the initiation of gust penetration and the lift asymptotically builds to the steady-state (circulatory) result (see Fig. 1).

For the subsonic compressible flow case, the two-dimensional sharp-edged gust response $\psi_g(s, M)$ was examined by Lomax[24] using a similar approach to that described in Ref. 21 to derive the indicial responses caused by changes in airfoil angle of attack and pitch rate. The subsonic gust result was also obtained in approximate form as a sum of exponential functions by Heaslet and Spreiter[25] using the reciprocal relations. One should note that if the gust function $\psi_g(s, M)$ is determined in appropriate analytic form, there are powerful numerical methods that can be applied to solve the Duhamel superposition integral to find the resulting airloads caused by an arbitrary gust field.

Lomax's solution to the sharp-edged gust problem was obtained from the two-dimensional wave equation using the

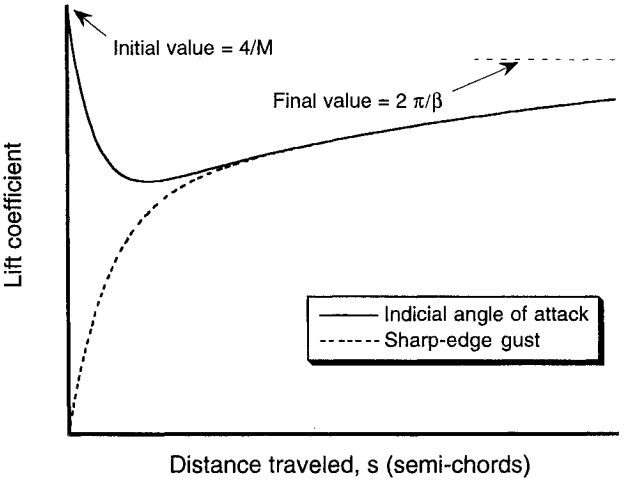

Fig. 1 Generic comparison of subsonic indicial angle of attack and sharp-edged gust solutions for unit magnitude changes in the boundary conditions.

method of supersonic analogy and subject to the appropriate boundary conditions. The actual calculations are fairly involved, but exact analytical expressions for the airfoil pressure distribution can be found for a limited period of time after the gust entry. For the period $0 \leq s \leq 2M/(1 + M)$, the airfoil pressure distribution for a unit gust disturbance is given exactly by

$$\Delta C_p(x, \hat{t}) = \frac{8}{\pi(1 + M)} \sqrt{\frac{M(\hat{t} - x)}{x + M\hat{t}}} \tag{1}$$

where x is measured from the airfoil leading edge and $\hat{t} = at$. When integrated, this expression yields for the normal force for a unit gust

$$\Delta C_n^s(s) = 2s/\sqrt{M} \tag{2}$$

where, by convention, s represents the distance traveled by the airfoil into the gust.

One interesting result from Eq. (2) is that the effect of increasing Mach number is to decrease the initial rate of lift production for a given distance traveled during the gust penetration. A similar result is found for the indicial angle-of-attack case, where there is an increasing lag in the development of the circulatory lift for higher subsonic Mach numbers.[20] It will also be seen from Eq. (2) that the lift builds rapidly during the gust penetration, and reaches close to one-third of its final value of $2\pi/\beta$ per radian shortly after the airfoil becomes fully immersed in the gust ($s = 2$).

For later values of time up to $s = 4M/(1 - M^2)$, solutions for the airfoil pressure distribution during the gust penetration are also known exactly from Ref. 24. Here, the chordwise pressure loading takes a more complicated form, namely

$$\Delta C_p(x, \hat{t}) = \frac{8}{\pi(1 + M)} \left\{ \sqrt{\frac{M(\hat{t} - x)}{x + M\hat{t}}} + \frac{2}{\pi} \sqrt{M(\hat{t} - x)(c - x - M\hat{t})} \left[\frac{2K}{\sqrt{(\hat{t}^2 - x^2)(1 - M^2)}} + \frac{EF'(\Psi) + KE'(\Psi) - KF'(\Psi)}{\sqrt{(x + M\hat{t})(c - x - M\hat{t})}} \right] \right\} \tag{3}$$

where E, K, $E'(\Psi)$, and $F'(\Psi)$ are elliptic integrals of various kinds with modulus k given by

$$k = \sqrt{\frac{(\hat{t} + x)(1 + M) - 2c}{(\hat{t} + x)(1 + M)}} \tag{4}$$

and argument $\Psi = \sin^{-1}\sqrt{(x + M\hat{t})/c}$. The integration of these equations to find the lift (and moment) is only possible by means of numerical methods. However, from the resulting pressure distributions the c.p. is found to reach the one-quarter-chord by $s = 2M/(1 + M)$ and remain there.

Later Values of Time

For $s > 4M/(1 - M^2)$ no exact solutions to the sharp-edged gust problem are possible in subsonic flow by means of the linear theory and more approximate methods must be adopted (see Lomax et al.[21] and Lomax[24]). Mazelsky[26] has used a relationship between ψ_g and the indicial response to a step change in angle of attack ϕ_α. Based on the small-disturbance theory of vortex sheets in a compressible fluid,[27] the result is

$$\psi_g(s, M) = \frac{1}{\pi} \int_0^2 \phi_\alpha(s - \sigma, M) \sqrt{\frac{\sigma}{2 - \sigma}}\, d\sigma \qquad s > 2 \tag{5}$$

The preceding equation can be used to find the intermediate variation in the gust response from the corresponding variation in the indicial response. This latter result is known, albeit also approximately in subsonic flow, from the work of various authors including Mazelsky,[26,28] and more recently, Leishman.[29] The solutions of Mazelsky are based on linear theory, whereas the solutions of Leishman are based on both exact linear theory and on various experimental measurements. Since the indicial response cannot be simulated experimentally, unsteady measurements on oscillating airfoils were used in Ref. 29 to relate back to find the indicial responses. While there are quantitative differences between the two methods, the qualitative behavior in respect to variations in Mach number is the same.

Direct Indicial Simulation by CFD

CFD solutions provide results for problems that cannot be solved analytically or simulated by experimentation. However, these solutions are only available at enormous computational cost, and even then are still subject to certain approximations and limitations. Nevertheless, CFD solutions can help establish results for model problems that would otherwise remain intractable. CFD indicial type calculations are rare in the published literature, but some nonlinear indicial and gust solutions have been performed[30–32] using various small-disturbance, full-potential, and Euler solvers.

A series of more elaborate indicial calculations has recently been performed by Parameswaran,[33] who has computed indicial angle of attack, pitch rate, and sharp-edged gust results using a Euler/Navier–Stokes method with a grid velocity approach. These results were computed using a two-dimensional version of the transonic unsteady rotor Navier–Stokes (TURNS) code, which is described in Ref. 34. These particular results are extremely useful since they help establish the bounds of linear theory, and also provide good check cases for the indicial method over a range of conditions where exact analytical solutions are mostly unavailable.

Computed CFD results for the sharp-edged gust problem are shown in Fig. 2 for Mach numbers of 0.3 and 0.5, and are compared to the exact linear theory obtained from Eq. (2) and the integration of Eq. (3). The comparisons are excellent, and lend significant credibility to the CFD results.

Functional Approximations to Gust Response

A key factor in the successful application of indicial-type methods to arbitrary gust (or other input) problems is the functional form used for the response function. Because of the asymptotic nature of the indicial functions, Mazelsky,[26] and Mazelsky and Drishler[28] have obtained exponential approximations to the stationary sharp-edged gust function. While the exponential behavior of the indicial function is not an exact representation of the physical behavior, it is sufficiently close

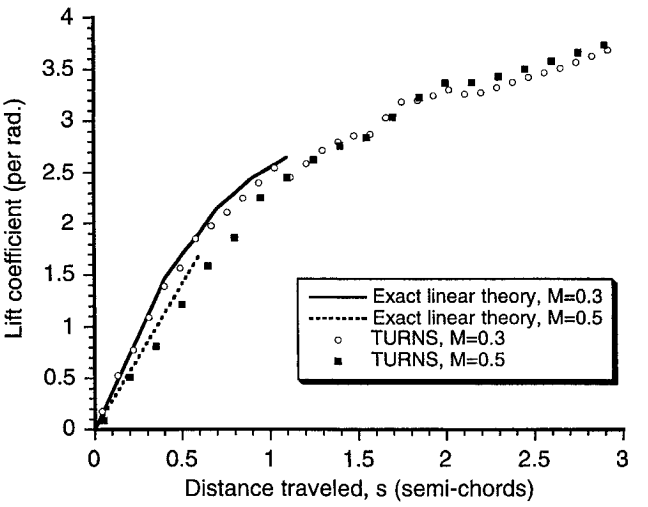

Fig. 2 Comparison of exact linear theory and CFD result for the penetration of a sharp-edged gust, M = 0.3, and 0.5.

for practical calculations. The exponential form also has a simple Laplace transform, thereby facilitating numerical computations for arbitrary forcing. This Duhamel superposition process can be performed by various techniques, as will be described. However, for some applications the exponential approximation to the indicial response may be inadequate, and caution should be used.

A typical exponential approximation for the sharp-edged gust is of the form

$$\psi_g(s, M) \approx 1 - \sum_{i=1}^{N} G_i(M)\exp[-g_i(M)s] \qquad s \geq 0 \quad (6)$$

where, as shown,[21] the G_i and g_i coefficients will, in general, all be Mach number dependent, but with $\Sigma_{i=1}^{N} G_i = 1$ and $g_i > 0$ for $i = 1 \ldots N$. The corresponding lift during the penetration of a sharp-edged gust of unit magnitude is given by

$$\Delta C_n^g(t, M) = (2\pi/\beta)\psi_g(s, M) \quad (7)$$

The steady-state value of the lift is simply the two-dimensional flat-plate result with the Glauert correction. For practical engineering calculations it is possible to replace the linearized value of the steady lift-curve-slope $2\pi/\beta$ in Eq. (7) by a value measured from experiment for any particular airfoil.

While the form of the exponential approximation in Eq. (6) may be acceptable for applications in fixed-wing analyses (if the approximating gust function coefficients at a given Mach number can be suitably obtained), it is inconvenient for a helicopter rotor analysis. This is because each blade station encounters a different local Mach number as a function of both blade radial location and azimuth angle. Therefore, repeated interpolation of the G_i and g_i coefficients between successive Mach numbers will be required to find the locally effective gust function. While simple in concept, there is a relatively large computational overhead associated with this type of repeated interpolation process, and the repetitive reinsertion of the relevant coefficients in the superposition algorithm. In addition, it must be recognized that when superposition is applied to the gust function to find the lift for an arbitrary field, each exponential term in the series in Eq. (6) contributes an additional overhead. Since this process will be applied at many discrete blade elements, the number of exponential terms in the approximation must be minimized.

It has been shown[29,35] that the asymptotic (circulatory) part of the total lift from a step change in angle of attack in subsonic compressible flow can be approximated by a two-term exponential function, and for all subsonic Mach numbers the results are related through a characteristic time that can be scaled in terms of Mach number alone. Since for later values of time it is known[20] that the sharp-edged gust and indicial angle-of-attack functions approach each other, it is sensible to assume a similar behavior for the sharp-edged gust function, i.e.,

$$\psi_g(s, M) \approx 1 - \sum_{i=1}^{N} G_i \exp(-g_i\beta^2 s) \qquad s \geq 0 \quad (8)$$

where $1 - \Sigma_{i=1}^{N} G_i = 0$, as before, but now the G_i and g_i are fixed and considered independent of Mach number. It will be shown that the form of this equation is valid up to at least the critical Mach number of the airfoil section, after which nonlinear effects may be expected because of the development of transonic flow. Also, note that if this simple compressibility scaling approach given by Eq. (8) can be justified for the sharp-edged gust function, it turns out to be not only more computationally efficient, but also more accurate than repeated linear interpolation of the G_i and g_i coefficients between discrete Mach numbers for which the gust function coefficients may be known.

Determination of $\psi_g(s, M)$ from Linear Theory

It is desirable to find the coefficients of the exponential approximations for the sharp-edged gust response using both the exact linear theory and CFD results, where available. The solution for the coefficients can be formulated as a least-squares optimization problem with several imposed constraints. To obtain an approximation to the exact linear theory, one constraint is imposed by matching the exact and approximate values of the time rate-of-change of lift at $s = 0$. This helps constrain the solution to ensure that the exact result will always be closely obtained in the initial stages. This part of the response is particularly important for transient aerodynamic phenomena such as BVI, which produces sound pressure levels at higher frequencies. (Recall that the final value theorem relates the response at infinite frequency to the initial value of the indicial response.)

The exact solution for the lift on the airfoil during the penetration of a sharp-edged gust of unit magnitude has been given previously in Eq. (2), and the approximation by Eq. (7). Differentiating these equations with respect to s and equating their gradients at $s = 0$ leads to a definition for the first constraint, namely

$$\sum_{i=1}^{N} G_i g_i = \frac{1}{\pi\sqrt{M\beta}} = \text{const at } s = 0 \quad (9)$$

Obviously, this cannot be obtained over the entire subsonic Mach number regime. However, an evaluation of the right-hand side of Eq. (9) shows that it is numerically close to 0.6 over the range $0.2 \leq M \leq 0.8$. As $M \to 0$, the slope tends to infinity at $s = 0$, which is consistent with the exact incompressible solution given by von Kármán and Sears.[17]

A second, and more rigorous, constraint is for the initial conditions, namely that

$$\sum_{i=1}^{N} G_i - 1 = 0 \quad (10)$$

In addition to the foregoing, we must impose that

$$G_i, g_i > 0, \qquad i = 1, 2 \ldots N \quad (11)$$

Finally, we know that as $s \to \infty$, the airloads approach the value given by the usual steady-state subsonic linearized airfoil theory, i.e., for a gust of unit magnitude

$$C_n^g(s = \infty, M) = 2\pi/\beta \quad (12)$$

A $2N$-dimensional vector of unknown coefficients can now be defined as

$$\boldsymbol{G}^T = \{G_1 \quad G_2 \ldots G_N \quad g_1 \quad g_2 \ldots g_N\} \quad (13)$$

The vector in Eq. (13) can be chosen to minimize the differences between the approximating exponential gust function and the exact or semiexact or CFD solutions over the domain of s and M for which results are available. Recall that we seek a single generalized gust function in terms of $2N$ coefficients, whose exponents g_i, $i = 1, N$ can be scaled by β^2 for application to different Mach numbers. As described previously, it is also possible to use results from the indicial angle-of-attack case to help find the asymptotic behavior of the gust response as $s \to \infty$.

An objective function $\bar{J}(\boldsymbol{G})$ can be defined as

$$\bar{J} = \sum_{i=1}^{I} w_i J(\boldsymbol{G}, M_i) \quad (14)$$

where

$$J(\boldsymbol{G}, M_i) = \sum_{m=1}^{M} [C_n^g(M_i) - C_n^g(\boldsymbol{G}, M_i)]^2 \quad (15)$$

The minimum of $\bar{J}$ in the parameter space $\boldsymbol{G}$ will give the best approximation to the exact linear theory over the domain of s and $0.2 < M \leq 0.8$.

The objective function minimization of $\bar{J}(\boldsymbol{G})$ in the parameter space $\boldsymbol{G}$ is subject to the constraints defined previously. The equality constraints may be replaced by the penalty functions, i.e.,

$$P_1(\boldsymbol{G}) = R_1 \left(\sum_{i=1}^{N} G_i - 1 \right)^2 \quad (16)$$

$$P_2(\boldsymbol{G}) = R_2 \left(\sum_{i=1}^{N} G_i g_i - \frac{1}{\pi\sqrt{M}\beta} \right)^2 \quad (17)$$

where R_1 and R_2 are penalty parameters. Thus, we obtain the pseudo-objective function

$$\tilde{J} = \sum_{i=1}^{I} w_i J(\boldsymbol{G}, M_i) + P_1(\boldsymbol{G}) + P_2(\boldsymbol{G}) \quad (18)$$

which is then minimized to obtain the gust function coefficients $\boldsymbol{G}$.

An optimization method was used to find the $\boldsymbol{G}$ coefficients in Eq. (8). Exact results for the gust response were computed at Mach numbers of 0.3, 0.5, and 0.8 using the solutions given by Eq. (2) and by the numerical integration of Eq. (3) up to $s = 4M/(1 - M^2)$. For the higher Mach number this corresponds to finding an exact solution up to 8.88 semichord lengths of airfoil travel, but this likely represents the highest Mach number for which linear theory is applicable. At $M = 0.3$, exact results can be computed only for the short period of 1.32 semichords. Asymptotic results for $s > 10$ for $M = 0.3$, 0.5, and 0.8 were computed using Eq. (5) with the indicial response caused by angle of attack. The weighting terms w_i were set to unity for the results for the exact theory, and to 0.75 for the asymptotic results computed from Eq. (5). There could also be some advantage in weighting the results for higher Mach numbers, for example, perhaps to allow for some nonlinear effect.

During the optimization process it was found that for $N = 1$ unacceptably large cost functions resulted, rendering this lowest-order approximation useless. On the other hand, the $N = 3$ case produced approximately the same cost function as for the $N = 2$ case. Because it is desirable to minimize the number of coefficients, and thereby the number of states or deficiency functions for numerical cost reasons, the $N = 2$ case was selected. The final results are shown for Mach numbers of 0.5 and 0.8 in Fig. 3. It will be seen that the approximations match the exact solutions almost precisely. The resulting coefficients are given in Table 1. A summary of the gust responses for extended values of time is shown in Fig. 4, where it is apparent that while the final values increase with increasing Mach number, the initial growth in lift is less.

Note from Table 1 that the values obtained in the present work for the coefficients of the generalized subsonic gust function as $M \to 0$ are close to those given by Jones for the exponential approximation to the incompressible Küssner function.[20] This confirms that the results for the subsonic case are closely approximated by scaling the g_i coefficients by β^2; that is, the aerodynamic gust responses are related in subsonic flow, albeit approximately, through a characteristic time.

Determination of $\psi_g(s, M)$ from CFD

Sharp-edged gust results were computed in Ref. 23 using the CFD analysis for a NACA 0012 airfoil at $M = 0.3$, 0.5, 0.65, and 0.8. A grid velocity approach was used to introduce the gust velocity field. For the higher Mach number, there was evidence of some nonlinearity (caused by the development of a shock wave on the upper surface of the airfoil), so that indicial coefficient results were obtained with a nonequal weighting to the data. Again, the optimization process confirmed that the $N = 2$ case gave a good overall approximation to the computed data. Like the exact linear theory, the time-scaling of the gust function by the factor β^2 appeared to be a feature confirmed by the CFD analysis, at least in the subsonic flow regime. The resulting coefficients for this generalized sharp-edged gust function are given in Table 1, and the results are plotted graphically in Fig. 5. The level of agreement of the exponential indicial approximation with the TURNS results is good, bearing in mind that this indicial function is generalized in terms of Mach number alone.

Table 1 Summary of sharp-edge gust function coefficients

Guest function	G_1	G_2	g_1	g_2
$\psi(s)$ (Ref. 20)	0.5	0.5	0.130	1.0
$\psi(s, M)$ (linear)	0.527	0.473	0.100	1.367
$\psi(s, M = 0.5)$ (linear)	0.527	0.473	0.075	1.025
$\psi(s, M)$ (CFD)	0.670	0.330	0.1753	1.637

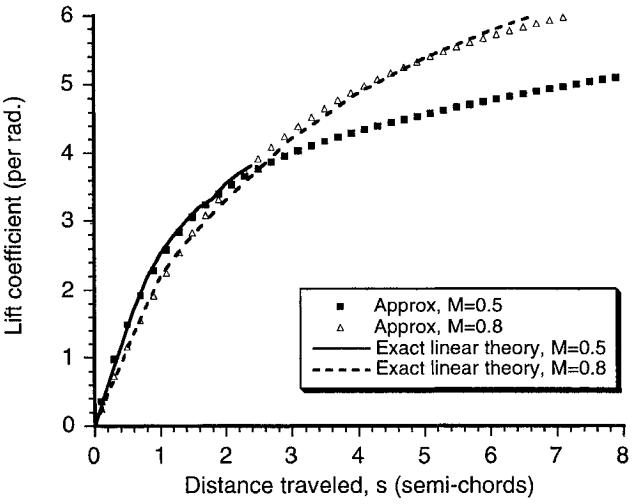

Fig. 3 Comparison of generalized exponential gust approximation with exact solutions given by subsonic linear theory for M = 0.5 and 0.8.

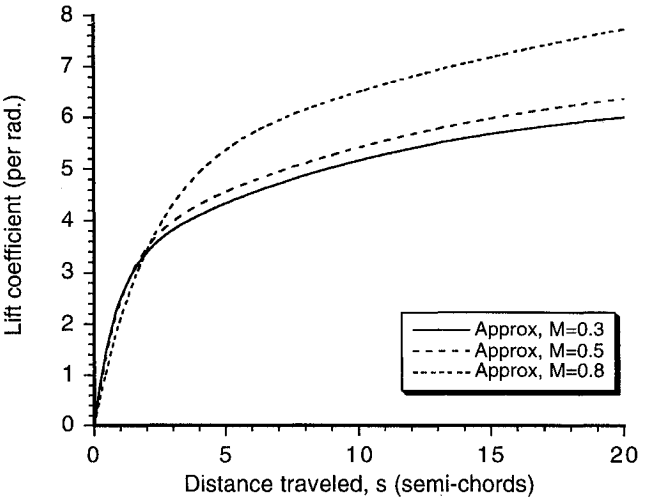

Fig. 4 Summary of generalized sharp-edged gust response for different Mach numbers.

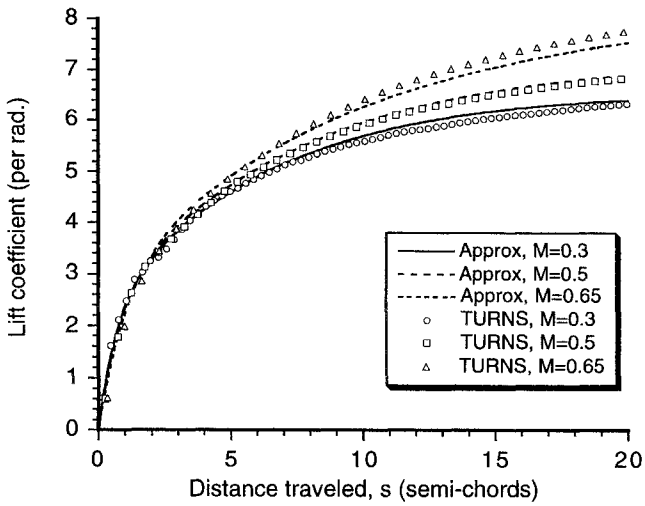

Fig. 5 Comparison of generalized approximations with TURNS at M = 0.3, 0.5, and 0.65.

Response to an Arbitrary Gust

Within the assumptions of the linear theory, a general stationary gust field $w_g(x, t)$ can be decomposed into a series of sharp-edged gusts of small magnitude. Using the indicial response for a sharp-edged gust, the response to an arbitrary gust field can be found using linear superposition in the form of Duhamel's integral. For example, the response to a continuous gust field may be written as

$$\Delta C_n^g(s) = \frac{2\pi}{\beta}\left[\frac{1}{V}\int_0^s \frac{dw_g}{d\sigma}\,\psi_g(s-\sigma, M)\,d\sigma\right] \tag{19}$$

where it is assumed that the in-plane velocity produces only a quasisteady effect. While the linearity of an arbitrary gust problem cannot necessarily be established a priori, especially for Mach numbers above the critical Mach number, the technique has been well proven using experimental measurements for oscillating airfoils in Refs. 29 and 35 for the Mach numbers typical of helicopter rotors, as well as for control surface deflections.[23,36]

The Duhamel superposition can be performed numerically in various ways, including the state-space (continuous time) form, or the one-step recursive formulation (discrete time) form. Both numerical approaches are useful for application inside a comprehensive rotor analysis, the former more so for active control or aeroelasticity problems. Because of its higher overall computational speed, the latter method is usually used in comprehensive rotor codes.

By the application of Laplace transforms to the exponential approximation to the sharp-edged gust function in Eq. (8), the lift transfer function relating the output (lift) to the input (the vertical gust velocity) can be obtained. For N = 2 (see later) the lift transfer function is

$$\Delta C_n^g(p) = \frac{2\pi}{\beta}\left(\sum_{i=1}^{N}\frac{G_i}{1+D_i p}\right) \tag{20}$$

where $D_i = c/(2Vg_i\beta^2)$. From this transfer function, the state-space form of the equations can be written in the form $\dot{z} = \boldsymbol{A}z + \boldsymbol{B}u$ where

$$z = [z_1(t) \quad z_2(t)]^T \tag{21}$$

$$\boldsymbol{A} = \begin{bmatrix} 0 & 1 \\ -g_1g_2(2V/c)^2\beta^4 & -(g_1+g_2)(2V/c)\beta^2 \end{bmatrix} \tag{22}$$

$$\boldsymbol{B}u = [0 \quad 1]^T\left[\frac{\Delta w_g(t)}{V}\right] \tag{23}$$

The corresponding output equation for the total lift coefficient caused by the arbitrary gust field is

$$\Delta C_n^g(t) = \frac{2\pi}{\beta} \qquad \boldsymbol{C}z = \frac{2\pi}{\beta}\,\alpha_e(t) \tag{24}$$

where the output matrix is

$$\boldsymbol{C} = [g_1g_2\beta^4(2V/c)^2 \quad (G_1g_1 + G_2g_2)\beta^2(2V/c)] \tag{25}$$

and α_e can be considered as an effective angle of attack. Note that the aerodynamic states, z_1 and z_2 (one for each exponential term in the indicial function), contain all of the information about the past history of the unsteady aerodynamic loads caused by the imposed gust field. These equations can then be solved using any standard ordinary differential equation solver for any arbitrarily imposed gust field.

For discrete time, a finite difference approximation to the Duhamel integral leads to a one-step recursive formulation, and the various numerical procedures were initially developed in Ref. 35 for airfoil motion using the indicial function concept. These methods can also be extended to the gust problem. For example, denoting the current sample by t and the nondimensional sample interval by Δs, the lift may be constructed from an accumulating series of small gust inputs using

$$\Delta C_{n_t}^g = (2\pi/\beta)(1/V)[\Delta w_{g_t} - Z_{1_t} - Z_{2_t}] = (2\pi/\beta)\alpha_{e_t} \tag{26}$$

Again, the N = 2 case has been assumed. The terms Z_{1_t} and Z_{2_t} are called deficiency functions, which like the aerodynamic states described previously, contain all of the time–history information about the aerodynamic forces. In this case, the deficiency functions are given by the one-step recursive formulas

$$Z_{1_t} = Z_{1_{t-1}}E_1 + G_1(\Delta w_{g_t} - \Delta w_{g_{t-1}}) \tag{27}$$

$$Z_{2_t} = Z_{2_{t-1}}E_2 + G_2(\Delta w_{g_t} - \Delta w_{g_{t-1}}) \tag{28}$$

where $E_1 = \exp(-g_1\beta^2\Delta s)$ and $E_2 = \exp(-g_2\beta^2\Delta s)$, and where the subscripts t and $t-1$ are the current and previous time steps, respectively.

Results and Discussion

Sinusoidal Gust

From the sharp-edge gust response, results can be computed for the aerodynamic response caused by a stationary sinusoidal gust, i.e., $w_g(x, t) = \sin(\omega_g t - \omega_g x/V)$. This is a classical problem in unsteady aerodynamics, and was solved exactly for incompressible flow by Sears.[37] The subsonic case has been evaluated by Graham[38] using similarity rules, and also by Osborne[39] and Filotas[40] using various other levels of approximation.

By the application of Laplace transforms the unsteady lift transfer function for the two-dimensional case can be obtained, as given previously by Eq. (20). There are two cases of interest. First, if the gust is referenced to the airfoil leading edge then x = 0, and so $w_g(t) = \sin(\omega_g t)$. If the gust is referenced to the midchord, then $x = c/2$ and the forcing becomes $w_g(t) = \cos(k_g)\sin(\omega_g t) - \sin(k_g)\cos(\omega_g t)$, which is equivalent to a phase shift. The midchord was the reference point used in the original work of Sears.[37]

Results for a sinusoidal gust referenced to the airfoil midchord have been computed for M = 0.2, 0.4, and 0.6 using the indicial coefficients obtained from the approximation to the exact linear theory. It can be seen from Fig. 6 that an interesting spiral curve is obtained, which for all Mach numbers is qualitatively similar to the incompressible case described by Sears.[37] (When the gust is referenced to the leading-edge of the airfoil, a function is obtained that looks somewhat similar to the Theodorsen function, as described by Kemp[41] and Gies-

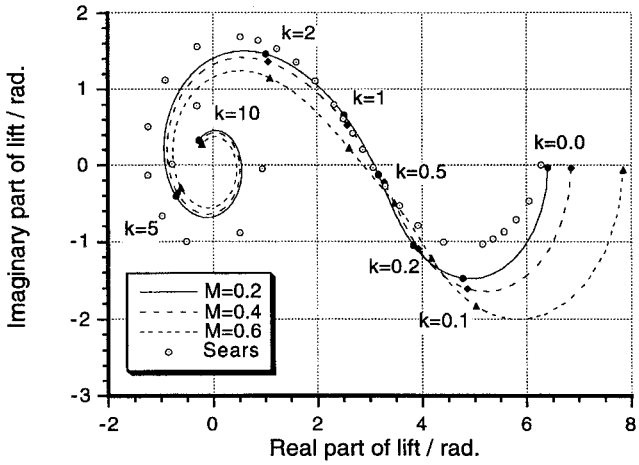

Fig. 6 Effect of compressibility on the lift for a sinusoidal gust.

ing et al.[42]) Figure 6 shows that the spiral tightens with increasing gust frequency producing a reduction in lift amplitude and a change in phase. Also, it appears from Fig. 6 that compressibility affects the phase of the lift response more at a given gust frequency rather than the amplitude, except in the low-frequency or quasisteady region where there is both an amplitude and phase effect.

Two-Dimensional BVI Problem

Comparison with CFD Solution

CFD calculations were made using TURNS[34] to obtain the unsteady loads on a NACA 0012 airfoil interacting with a convecting vortex of nondimensional strength $\hat{\Gamma} = 0.2$ traveling at a steady velocity 0.26 chords ($y_v = y_0 = -0.26c$) below the airfoil. Typical helicopter advancing blade conditions at Mach numbers between 0.5–0.8 were considered, since these two conditions serve to illustrate the significant influence of compressibility on the BVI problem. The CFD results were compared to solutions obtained using the indicial approach, which although restricted here to the calculation of the integrated airloads, has a relative computational speed advantage of about 10^5.

The tangential velocity in the interacting vortex was approximated as[43]

$$V_\theta(r) = \frac{\Gamma r}{2\pi(r_c^{2n} + r^{2n})^{1/n}} \tag{29}$$

where n is an integer variable, and r is the distance along a radial line emanating from the center of the vortex so that $r^2 = (x - x_v)^2 + (y - y_v)^2$, and x_v, y_v relative to a coordinate axis at the leading edge of the airfoil. A value of $n = 1$ (Kaufmann or Scully vortex) was used for the vortex model with $r_c = 0.05c$, although the interaction between the airfoil and the vortex is sufficiently spaced in the cases considered so that the core radius does not play a significant role. The reciprocal influence of the airfoil on the vortex convection velocity and trajectory was neglected.

Results for two subsonic Mach numbers and for a weakly transonic case are shown in Fig. 7. It can be seen that the influence of the vortex has affected the airfoil lift when it is well upstream of the airfoil leading edge. This result is important for the computations because it sets a minimum upstream distance to establish the initial conditions for both the CFD and indicial approaches. A lift minimum was obtained just as the vortex passed the airfoil leading edge, followed by a rapid increase in the lift as the vortex passed downstream over the chord. Note that the agreement between the indicial approach and the TURNS code is excellent at the subsonic Mach numbers, and these results essentially confirm the validity of linear theory under these conditions.

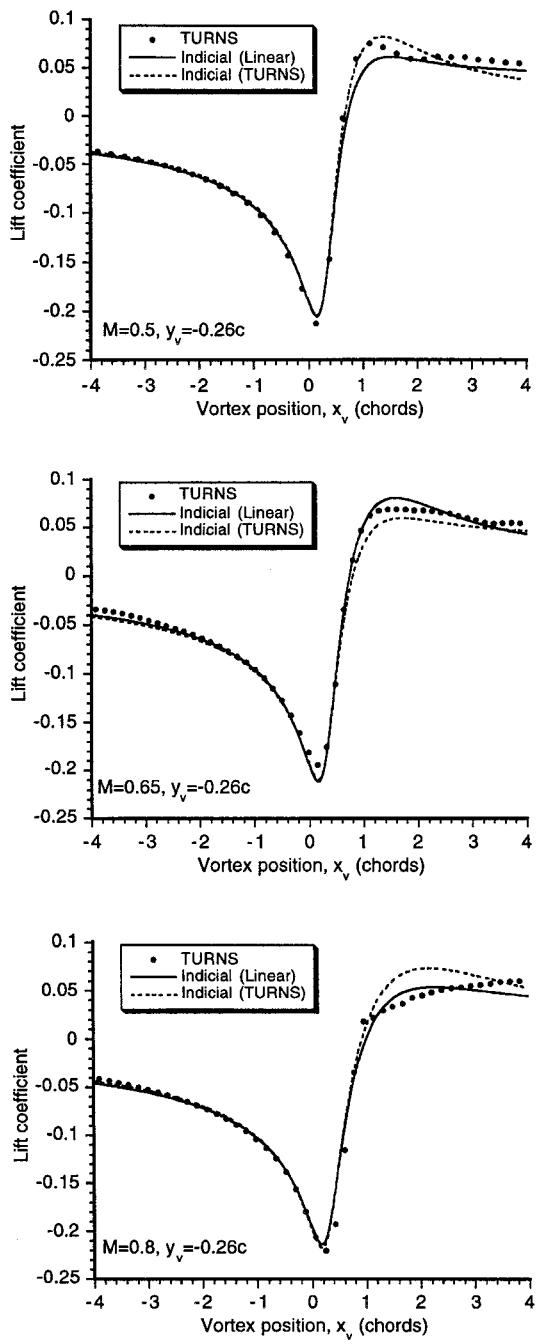

Fig. 7 Comparison with TURNS result for a two-dimensional vortex-airfoil interaction, $\hat{\Gamma} = 0.2$ and $y_0 = -0.26$ for $M = 0.5, 0.65,$ and 0.8.

Even for the higher Mach number of 0.8, which mildly exceeds the critical Mach number of this NACA 0012 section so that some nonlinearities caused from the transonic nature of the flow are expected, the agreement in terms of peak-to-peak lift and phasing is good. However, the lower part of Fig. 7 shows that there is a somewhat larger lift overshoot downstream of the airfoil trailing edge compared to that predicted by TURNS. This is because of weak transonic effects, and was evident in the computed pressure distributions where the forward propagation of pressure disturbances from the trailing-edge region were delayed by the local supersonic pocket on the airfoil upper surface.

Also, it will be seen from the results in Fig. 7 that the effects of increasing Mach number serves to attenuate the peak-to-peak value of the lift response, which is exactly opposite to that given by incompressible unsteady theory. Furthermore, it

is apparent that the effects of increasing Mach number introduce a larger phase lag in the lift response (the slope is less during the interaction), and this obviously becomes a significant consideration when accurate noise predictions are an issue.

Comparison with Experiment

Experimental investigations of the idealized two-dimensional BVI problem are rare. This is not surprising bearing in mind the difficulties in controlling the development of the vortex and preserving the two-dimensional nature of the interaction. In the work of Straus et al.,[44,45] a nominally two-dimensional vortex was generated from a pitching wing upstream, and this vortex was allowed to convect downstream and interact with a two-dimensional NACA 0012 airfoil at a fixed angle of attack. While this BVI-type encounter can be classified as nominally two dimensional, three-dimensional effects must be present to some (although undocumented) degree. Also, it should be noted that the flow Mach number and Reynolds number in the experiment were much lower compared to that obtained in the rotor environment.

The first case was for counterclockwise $\hat{\Gamma} = -0.15$, and vertical miss-distance $y_v = y_0 = -0.24c$. Referring to the upper part of Fig. 8, a lift maximum was obtained just as the vortex passed the leading edge, followed by a sharp reduction in the lift as the vortex passed downstream over the chord. The calculations made using the indicial method were found to compare quite well with the test data for the peak-to-peak lift and, perhaps more importantly for acoustics, the phasing of the lift response during the vortex encounter. The second case was for a slightly closer interaction and with a vortex rotation in the opposite (clockwise) sense, i.e., $\hat{\Gamma} = 0.16$, $y_v = y_0 = -0.19c$. As shown in the lower of Fig. 8, in this case the lift reduced to a negative peak as the vortex approached the airfoil leading edge. Compared to the previous case, however, some discrepancies were noted as the vortex passed the airfoil trailing edge. In this case, there was little lift overshoot after the interaction that was measured in the experiment. It is possible that viscous or three-dimensional effects play some role, and that the initially coherent vortex structure may have been modified after the interaction. Nevertheless, in both cases the agreement with test data is good in the critical region where the lift gradients and unsteady aerodynamic effects are greatest.

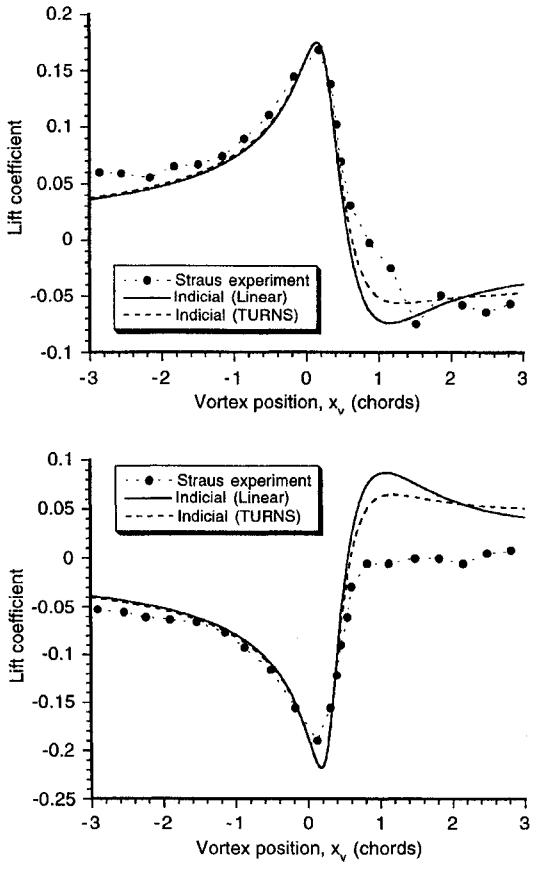

Fig. 8 Comparison with experimental data for a two-dimensional vortex-airfoil interaction. Upper plot for $\hat{\Gamma} = -0.15$ and $y_0 = -0.24c$. Lower plot for $\hat{\Gamma} = +0.16$ and $y_0 = -0.19c$.

Three-Dimensional Problem

The three-dimensional BVI problem is considerably more complicated, and identifying individual BVI events in the helicopter rotor environment to the point where validation of any aerodynamic model would be possible is extremely difficult. However, several simpler BVI experiments with rotors have been conducted in the controlled environment of wind tunnels.[46–49] All of these experiments are based on one- or two-bladed rotors with pressure-instrumented blades that encounter a controlled isolated vortex generated upstream of the rotor.

The recent work of Refs. 50 and 51 is extremely useful for validating the BVI aeroacoustics problem, because both unsteady blade loads and acoustic pressures were measured simultaneously. In this experiment, a two-bladed rotor with elastically stiff blades encountered a vortex (generated by a wing placed about three rotor radii upstream of the rotor shaft) of measured strength and location relative to the rotor. The BVI event took place over the front of the rotor disk, where the blade was effectively parallel to the longitudinal axis of the generator vortex. The rotor was operated at nominally zero thrust so that the effects of its self-generated wake on the blade loads and acoustics would be minimized.

The location of the generating vortex relative to the rotor (blade) was changed by adjusting the position of the generating wing, with the vortex sign and strength being changed by altering the wing angle of attack. For the present work, a nondimensional generator vortex strength of 0.36 was used with a viscous core size that was 5% of the generating wing chord, these parameters being based on the measurements of Takahashi and McAlister.[52] In addition, the tangential (swirl) velocity of the vortex has been found to closely correspond to the $n = 1$ case of the general profiles given by Eq. (29).

The unsteady airloads on the blade were measured by 60 pressure transducers distributed at three spanwise stations over the blade. The acoustics were measured by arrays of microphones located both in the near field (roughly 0.5 rotor radius away) and the far field (roughly three rotor radii away) relative to the rotational axis, with both microphone sets on the retreating side of the rotor.[50,51] Since the indicial approach requires integrated airloads, the chordwise pressures measured at the three radial blade locations were numerically integrated.

The unsteady airloads on the rotor were modeled by applying the indicial method at 25 radial stations along the blade, and including induced effects from the near trailed wake by means of a Wessinger L-type model. In this approach the three-dimensional spanwise loading (therefore including both trailed and shed wake effects) is computed by an influence function method, requiring the solution of a set of coupled linear simultaneous equations at each time step.

The acoustic pressures were calculated by using the acoustic analogy in the form of the Ffowcs Williams–Hawkins (FW–H) equation. In the present work Farassat's formulation-1 was used,[53,54] where the acoustic pressure can be written as

$$p'(\boldsymbol{x}, t) = \frac{1}{4\pi}\frac{\partial}{\partial t}\iint\left[\frac{\rho v_n}{\mathcal{R}(1 - M_{\mathcal{R}})}\right]_\tau \mathrm{d}S + \frac{1}{4\pi a}\frac{\partial}{\partial t}\iint\left[\frac{l_{\mathcal{R}}}{\mathcal{R}(1 - M_{\mathcal{R}})}\right]_\tau \mathrm{d}S + \frac{1}{4\pi}\frac{\partial}{\partial t}\iint\left[\frac{l_{\mathcal{R}}}{\mathcal{R}^2(1 - M_{\mathcal{R}})}\right]_\tau \mathrm{d}S \tag{30}$$

The first term in Eq. (30) is the thickness noise, the second two terms are the loading noise. The quadropole term has been neglected since in the Ames experiment the maximum local Mach number only briefly exceeds the critical Mach number of the airfoil section over a small part of the advancing blade tip. The retarded time equation was solved using a binning technique, which has the advantage of vastly increased computational speed using formulation-1 at the expense of some minor loss in accuracy.

Since the linearity assumptions of the indicial method do not allow for variations in the form of the chordwise pressure, an assumed pressure mode was used. For the noncompact calculation used in the present work a chordwise pressure loading was synthesized from the unsteady lift. In its simplest form this mode shape can be the (analytic) subsonic form or another (discretized) form as given by the CFD analysis that is then linearly scaled as a function of angle of attack and the Glauert factor. Similarly, the thickness loading was synthesized from a mode shape, this being derived from either the no-penetration condition on the airfoil surface (a NACA 0012 in this case) or from a (discretized) form generated by the CFD analysis. However, it was found that the acoustics pressures were insensitive to the assumed chordwise pressure modes, and even in the compact limit of a concentrated force dipole the predicted noise signatures were not unreasonable.

The predicted unsteady normal force coefficient at the three radial stations on the reference blade is shown in Fig. 9 for a negative vortex strength, and with the vortex passing 0.25 chords below the blade. Like the two-dimensional case, the airloads vary rapidly with respect to rotor azimuth position, changing sign as the blade passes from one side of the vortex to the other. Although the BVI event in this case is nominally parallel, successive parts of the blade encounter the vortex over a finite range of azimuth angles, with the interaction effectively sweeping from the root of the blade out toward the tip. Under these conditions some three dimensionality is produced, and this is apparent in the acoustics. However, the airloads over the extreme tip of the blade are critical and are responsible for the majority of the acoustics.

While the overall agreement of the predictions with test data was found to be good, there was a tendency to slightly overpredict the peak-to-peak amplitude of the unsteady airloads. Both the linear and CFD-based indicial functions were found to give essentially the same results, with the CFD indicial function giving a slightly less rapid buildup in lift after the interaction. However, it is the slope of the C_n curve or the time rate-of-change of the airloads during the interaction that is important from the perspective of the acoustics. Incompressible theory will always overpredict this slope. Note also that while the unsteady loads decrease in magnitude moving outward toward the tip, the BVI event takes place over a shorter

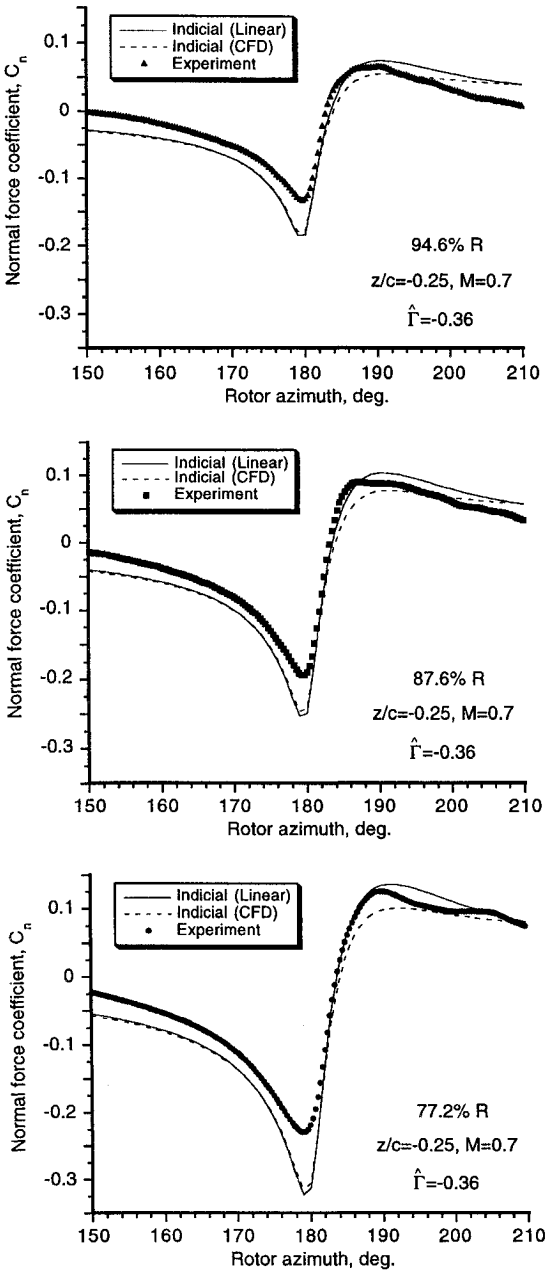

Fig. 9 Comparison of predicted and measured unsteady lift at three radial blade stations during BVI, $z/c = -0.25$ and $\hat{\Gamma} = -0.36$.

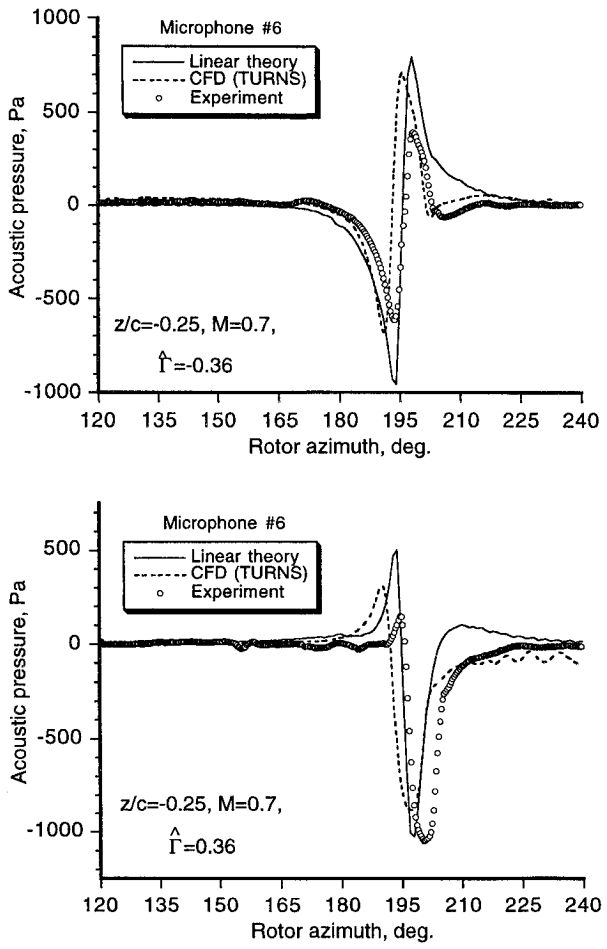

Fig. 10 Comparison of near-field acoustic pressures using linear theory and TURNS, $z/c = -0.25$ and $\hat{\Gamma} = \pm 0.36$.

time interval since the blade travels further in a given azimuth. Therefore, from an acoustics perspective, the outermost stations can be more important than stations just slightly further inboard that may carry more unsteady lift.

Both the near- and far-field acoustics are sensitive to the phasing of the unsteady airloads during the BVI. In addition, the duration and phasing of the BVI event along the blade, the Doppler magnification, and the distance of the event to the microphone location combine to produce the net sound pressure signature at a given time. The thickness sound pressure further combines with the loading term, resulting in small variations in phasing that can significantly affect the net noise signature. Sample predictions of the near-field sound pressure are shown in Fig. 10 and are compared with the acoustic pressure computed directly using the TURNS code, with further details given in Ref. 55. Note that both the CFD and linear methods overpredict the peak-to-peak pressures, but the TURNS code produces a better correlation with the test data at the trailing edge of the pulse. This is expected because of the more complicated nature of the flow physics on the blade during this region, which involves the upstream propagation of pressure disturbances from the trailing edge of the blade. This effect is not explicitly represented in the indicial method. Note that the acoustic pulse is received at the near-field microphone locations only about 10 deg after the BVI event. The slight phase shift in the CFD results is caused by a 0.11 chord lateral offset in the assumed location of the generator vortex, a fact that only became apparent after the calculations had been performed.

The far-field acoustics are considerably less in overall intensity, with the peak sound pressures being about 20 dB lower than in the near field. Referring to Fig. 11, note that the acoustic pressures take on the characteristic positive or negative going pulse (depending on the sign of the generator vortex) that has become well known as typical of a BVI event.[1,2] There are two acoustic pulses per rotor revolution since each blade interacts with the vortex 180 deg apart. Because of the lower intensity sound pressures, the far-field noise levels exhibit more noise, in part, because of reflections from the wind-tunnel walls. It will be seen that in the far field the pressure pulse is received some 140 deg of blade rotation after the BVI event. There was only a mild directivity for the four microphones in the far field, so that the magnitude of the sound pressure was much the same for all of the microphones. Note, however, that with the longer path length to microphone 5 compared to microphone 3, there is a measurable phase lag of about 20 deg of blade rotation in the arrival of the sound pulse. Figure 11 indicates that the current predictions are about 3 dB larger than the measured values, although the character of the signal (and therefore its frequency content) is captured very well with the indicial method.

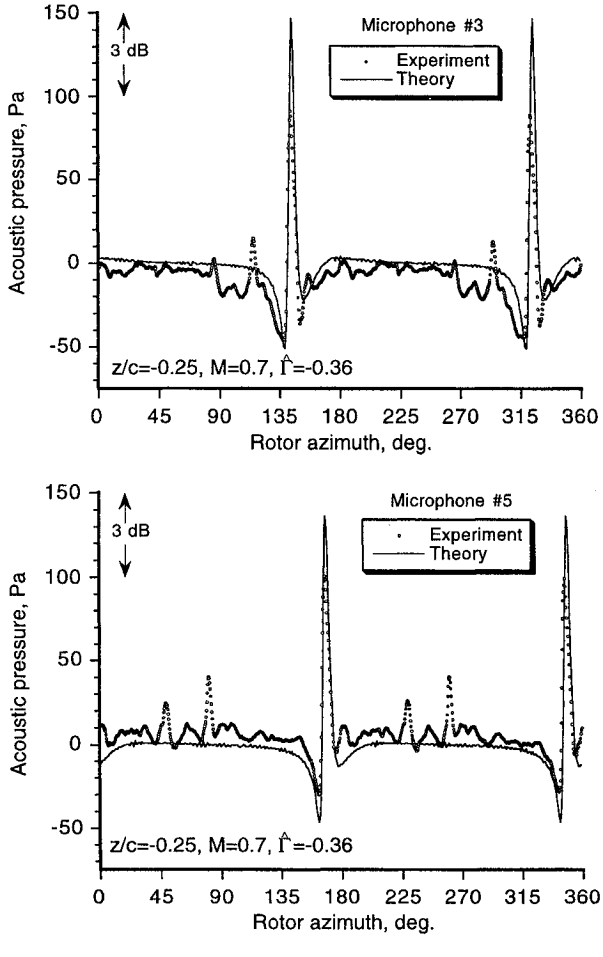

Fig. 11 Far-field acoustic pressures at microphones 3 and 5, $z/c = -0.25$ and $\hat{\Gamma} = -0.36$ (negative vortex).

Conclusions

An approach has been described to obtain functional approximations, generalized in terms of Mach number alone, to the unsteady lift on an airfoil penetrating a stationary sharp-edge gust in subsonic flow. Comparisons with experiments and CFD results have shown that it is feasible to compute accurately the unsteady lift on an airfoil during encounters with vortices in subsonic flow using indicial methods. It has been noted that compressibility affects both the magnitude and phasing of the unsteady airloads during a BVI encounter. Increasing the Mach number tends to decrease the peak-to-peak unsteady airloads in the high subsonic range, but accurate predictions of the phasing of the airloads with respect to vortex position is key to predicting the acoustics. When integrated into a three-dimensional rotor simulation, the indicial method provided good agreement with unsteady airloads measured on the blades during a BVI event. Both the near- and far-field acoustic pressures were found to be predicted to about a 3 dB accuracy. In all cases, the essential character of the acoustic signature was well represented. Along with the attractive computational benefits, such levels of correlation give considerable credibility to the indicial approach for aeroacoustic studies, and may form the basis for future work with active aeroacoustic control.

Acknowledgments

The author would like to thank Vasudev Parameswaran for running the sharp-edged gust calculations with TURNS. Thanks also go to James Baeder and Megan McCluer for helpful discussions on the BVI problem. The assistance of Francis Caradonna in providing the BVI airloads data and Cahit Kitaplioglu in providing the acoustics data are appreciated.

References

[1]Schmitz, F. H., "Rotor Noise, Aeroacoustics of Flight Vehicles: Theory and Practice," Vol. 1, NASA Reference Publication 1258, Aug. 1991, Chap. 2.

[2]Schmitz, F. H., and Yu, Y. H., "Helicopter Impulsive Noise: Theoretical and Computational Status," *Journal of Sound and Vibration*, Vol. 109, 1986, pp. 361–422.

[3]Widnall, S., "Helicopter Noise Due to Blade-Vortex Interaction," *Journal for the Acoustical Society of America*, Vol. 50, No. 1, Pt. 2, 1971, pp. 354–365.

[4]Nakamura, Y., "Prediction of Blade-Vortex Interaction Noise from Measured Blade Pressure Distributions," 7th European Rotorcraft Forum, Paper 32, Sept. 1981.

[5]Srinivasan, G. R., and McCroskey, W. J., "Numerical Simulations of Unsteady Airfoil Interactions," *Vertica*, Vol. 11, Nos. 1–2, 1987, pp. 3–28.

[6]Baeder, J. D., "Computation of Non-Linear Acoustics in Two-Dimensional Blade-Vortex Interactions," 13th European Rotorcraft Forum, Paper 1-1, Sept. 1987.

[7]Johnson, W., "A Comprehensive Analytical Model of Rotorcraft Aerodynamics and Dynamics," NASA TM-81182, June 1980.

[8]Chopra, I., and Bir, G., "University of Maryland Advanced Rotor Code: UMARC," American Helicopter Society Aeromechanics Specialists' Meeting, San Francisco, CA, Jan. 1994.

[9]Beddoes, T. S., "Unsteady Aerodynamics—Application to Helicopter Noise and Vibration Sources," AGARD Symposium on Unsteady Aerodynamics, Göttingen, Germany, May 1985.

[10]Johnson, W., "Calculation of Blade-Vortex Interaction Airloads on Helicopter Rotors," *Journal of Aircraft*, Vol. 26, No. 5, 1989, pp. 470–475.

[11]Dawson, S., "Wind Tunnel Test of an Active Flap Rotor: BVI Noise and Vibration Reduction," American Helicopter Society 51st Annual Forum, Fort Worth, TX, May 1995.

[12]Milgram, J., and Chopra, I., "Helicopter Vibration Reduction with Trailing Edge Flaps," American Helicopter Society Aeromechanics Specialists Meeting, Fairfield, CT, Oct. 1995.

[13]Tobak, M., and Schiff, L. B., "Aerodynamic Mathematical Modeling—Basic Concepts," *Dynamic Stability Parameters*, AGARD LS-114, 1981.

[14]Horlock, J. H., "Fluctuating Lift Forces on Airfoils Moving Through Transverse and Chordwise Gusts," *Journal of Basic Engineering*, Vol. 90, Series D, Dec. 1968, pp. 494–500.

[15]Van der Wall, B., and Leishman, J. G., "The Influence of Variable Flow Velocity on Unsteady Airfoil Behavior," *Journal of the American Helicopter Society*, Vol. 39, No. 4, 1994, pp. 288–297.

[16]Küssner, H. G., "General Airfoil Theory," NASA TM 979, 1941.

[17]Von Kármán, T., and Sears, W. R., "Airfoil Theory for Non-Uniform Motion," *Journal of the Aeronautical Sciences*, Vol. 5, No. 10, 1938, pp. 379–390.

[18]Miles, J. W. "The Aerodynamic Force on an Airfoil in a Moving Gust," *Journal of the Aeronautical Sciences*, Vol. 23, Nov. 1956, pp. 1044–1050.

[19]Drischler, J. A., and Diederich, F. W., "Lift and Moment Responses to Penetration of Sharp-Edged Traveling Gusts, with Application to Penetration of Weak Blast Waves," NACA TN 3956, May 1957.

[20]Bisplinghoff, R. L., Ashley, H., and Halfman, R. L., *Aeroelasticity*, Addison–Wesley, Reading, MA, 1955.

[21]Lomax, H., Heaslet, M. A., Fuller, F. B., and Sluder, L., "Two and Three Dimensional Unsteady Lift Problems in High Speed Flight," NACA Rept. 1077, 1952.

[22]Lomax, H., "Indicial Aerodynamics," *AGARD Manual on Aeroelasticity*, Oct. 1968, Chap. 6.

[23]Hariharan, N., and Leishman, J. G., "Unsteady Aerodynamics of a Flapped Airfoil in Subsonic Flow Using Indicial Concepts," AIAA Paper 95-1228, April 1995.

[24]Lomax, H., "Lift Developed on Unrestrained Rectangular Wings Entering Gusts at Subsonic and Supersonic Speeds," NACA TN 2925, April 1953.

[25]Heaslet, M. A., and Spreiter, J. R., "Reciprocity Relations in Aerodynamics," NACA Rept. 1119, Feb. 1952.

[26]Mazelsky, B., "Determination of Indicial Lift and Moment of a Two-Dimensional Pitching Airfoil at Subsonic Mach Numbers from Oscillatory Coefficients with Numerical Calculations for a Mach Number of 0.7," NACA TN 2613, Feb. 1952.

[27]Garrick, I. E., "On Some Fourier Transforms in the Theory of Nonstationary Flows," *5th International Congress for Applied Mechanics*, Wiley, New York, 1939, pp. 590–593.

[28]Mazelsky, B., and Drischler, J. A., "Numerical Determination of Indicial Lift and Moment Functions of a Two-Dimensional Sinking and Pitching Airfoil at Mach Numbers 0.5 and 0.6," NACA TN 2739, 1952.

[29]Leishman, J. G., "Indicial Lift Approximations for Two-Dimensional Subsonic Flow as Obtained from Oscillatory Airfoil Measurements," *Journal of Aircraft*, Vol. 30, No. 3, 1993, pp. 340–351.

[30]Stahara, S. S., and Spreiter, J. R., "Research on Unsteady Transonic Flow Theory," Neilson Engineering and Research Rept., NEAR TR-107, Jan. 1976.

[31]Ballhaus, W. F., and Goorjian, P. M., "Computation of Unsteady Transonic Flows by the Indicial Method," *AIAA Journal*, Vol. 16, No. 2, 1978, pp. 117–124.

[32]McCroskey, W. J., and Goorjian, P. M., "Interactions of Airfoils with Gusts and Concentrated Vortices in Unsteady Transonic Flow," AIAA Paper 83-1691, July 1983.

[33]Parameswaran, V., "Concepts for the Reduction of Blade Vortex Interaction Noise and the Use of CFD to Determine Indicial and Gust Responses of an Airfoil in Compressible Flow," Univ. of Maryland, Dept. of Aerospace Engineering, College Park, MD, Aug. 1995.

[34]Srinivasan, G. R., Baeder, J. D., Obayashi, S., and McCroskey, W. J., "Flowfield of a Lifting Rotor in Hover: A Navier-Stokes Simulation," *AIAA Journal*, Vol. 30, No. 10, 1992, pp. 2371–2378.

[35]Beddoes, T. S., "Practical Computation of Unsteady Lift," *Vertica*, Vol. 8, No. 1, 1984, pp. 55–71.

[36]Leishman, J. G., "Unsteady Lift of an Airfoil with a Trailing-Edge Flap Based on Indicial Concepts," *Journal of Aircraft*, Vol. 31, No. 2, 1994, pp. 288–297.

[37]Sears, W. R., "Some Aspects of Non-Stationary Airfoil Theory and Its Practical Application," *Journal of the Aeronautical Sciences*, Vol. 8, No. 3, 1941, pp. 104–108.

[38]Graham, J. M. R., "Similarity Rules for Thin Aerofoils in Non-Stationary Subsonic Flows," *Journal of Fluid Mechanics*, Vol. 43, Pt. 4, 1970, pp. 753–766.

[39]Osborne, C., "Unsteady Thin Airfoil Theory in Subsonic Flow," *AIAA Journal*, Vol. 11, No. 2, 1973, pp. 205–209.

[40]Filotas, L. T., "Oblique Compressible Sears Function," *AIAA Journal*, Vol. 12, No. 11, 1974, pp. 1601–1603.

[41]Kemp, N. H., "On the Lift and Circulation of Airfoils in Some Unsteady Flow Problems," *Journal of the Aeronautical Sciences*, Vol. 19, No. 10, 1952, pp. 713, 714.

[42]Giesing, J. P., Rodden, W. P., and Stahl, B., "Sears Function and Lifting Surface Theory for Harmonic Gust Fields," *Journal of Aircraft*, Vol. 7, No. 3, 1970, pp. 252–255.

[43]Vatistas, G. H., Kozel, V., and Mih, W. C., "A Simpler Model for Concentrated Vortices," *Experiments in Fluids*, Vol. 11, 1991, pp. 73–76.

[44]Straus, J., "Airfoil Pressure Measurements for a Two-Dimensional Blade-Vortex Interaction," M.S. Thesis, Rensselaer Polytechnic Inst., New York, 1986.

[45]Straus, P., Renzoni, P., and Mayle, R. E., "Airfoil Pressure Measurements During a Blade-Vortex Interaction and a Comparison with Theory," AIAA Paper 88-0669, Jan. 1988.

[46]Surendraiah, M., "An Experimental Study of Rotor Blade-Vortex Interaction," NASA CR-1573, May 1970.

[47]Caradonna, F. X., Laub, G. H., and Tung, C., "An Experimental Investigation of the Parallel Blade-Vortex Interaction," Workshop on Blade Vortex Interaction, NASA Ames Research Center, Moffett Field, CA, Oct. 1984.

[48]Kokkalis, T., and Galbraith, R. A., "Description of and Preliminary Results from a New Blade-Vortex Interaction Test Facility," 12th European Rotorcraft Forum, Paper 80, Garmish, Germany, Sept. 1986.

[49]Seath, D. D., Kim, J. M., and Wilson, D. R., "An Investigation of the Parallel Blade-Vortex Interaction in a Low Speed Wind-Tunnel," AIAA Paper 87-1344, June 1987.

[50]Kitaplioglu, C., and Caradonna, F. X., "Aerodynamics and Acoustics of Blade Vortex Interaction Using an Independently Generated Vortex," American Helicopter Society Aeromechanics Specialists Conf., San Francisco, CA, Jan. 1994.

[51]Kitaplioglu, C., Caradonna, F. X., and Burley, C. L., "Parallel Blade-Vortex Interactions: An Experimental Study and Comparison with Computation," American Helicopter Society Aeromechanics Specialists Conf., Bridgeport, CT, Oct. 1995.

[52]Takahashi, R. K., and McAlister, K. W., "Preliminary Study of a Wing-Tip Vortex Using Laser Velocimetry," NASA TM 88343, Jan. 1987.

[53]Farassat, F., "Linear Acoustic Formulas for Calculation of Rotating Blade Noise," *AIAA Journal*, Vol. 19, No. 9, 1981, pp. 1122–1130.

[54]Brentner, K. S., "Prediction of Helicopter Rotor Discrete Frequency Noise," NASA TM 87721, Oct. 1986.

[55]McCluer, M. S., and Baeder, J. D., "Comparison of Experimental Blade-Vortex Interaction Noise with Computational Fluid Dynamic Calculations," American Helicopter Society 51st Annual Forum, Fort Worth, TX, May 1995.